ISSN 1027-4510, Journal of Surface Investigation: X-ray, Synchrotron and Neutron Techniques, 2018, Vol. 12, No. 1, pp. 27–32. © Pleiades Publishing, Ltd., 2018.
Original Russian Text © G.S. Bocharov, A.V. Eletskii, A.V. Zakharenkov, O.S. Zilova, A.P. Sliva, E.V. Terentyev, S.D. Fedorovich, G.N. Churilov, 2018, published in Poverkhnost', 2018, No. 1, pp. 33–39.

Optimization of Steel-Surface Hardening by Carbon Nanostructures Followed by Treatment with High-Intensity Energy Sources

G. S. Bocharov[a], A. V. Eletskii[a], A. V. Zakharenkov[a], O. S. Zilova[a], A. P. Sliva[a], E. V. Terentyev[a], S. D. Fedorovich[a, *], and G. N. Churilov[b]

[a] *National Research University "Moscow Power Engineering Institute", Moscow, 111250 Russia*
[b] *Kirensky Institute of Physics, Siberian Branch, Russian Academy of Sciences, Krasnoyarsk, 660036 Russia*
**e-mail: FedorovichSD@mail.ru*

Received April 28, 2017

Abstract—The effect whereby a steel surface is modified by its covering with a nanocarbon material followed by fast electron- or laser-beam irradiation is studied. The initial material is low-carbon steel. Soot produced via the thermal sputtering of graphite electrodes in an electric arc with the subsequent extraction of fullerenes is used as the nanocarbon coating. Due to the fact that nanocarbon-coated samples are irradiated with a 60-keV electron beam, the material microhardness enhances considerably. The dependence between the microhardness and the irradiation energy is nonmonotonic and reaches its maximum (about 600 ± 20 HV) under the condition that the electron-irradiation energy is 460 J/cm^2 and the intensity is 1.53 kW/cm^2. This corresponds to a fourfold increase in the microhardness. Electron-beam irradiation of the treated surface is accompanied by a 1.5–2-fold decrease in the friction coefficient. Experimental results are compared with data obtained under laser irradiation of the nanocarbon-coated steel surface.

Keywords: metal surface hardening, carbon nanomaterials, laser irradiation, electron-beam treatment, microhardness

DOI: 10.1134/S102745101801007X

INTRODUCTION

The surface hardening of constructional materials is one of the key directions of modern materials science. The most widespread approaches to solving this problem involve a combination of a doping procedure and subsequent heat or mechanical treatment of surfaces (see, e.g., [1]). As a rule, the doping agents of constructional materials are Ni, Al, Si, Co, V, and Nb. In recent years, researchers have been interested in the possibility of creating hardening coatings based on similar structures in connection with the discovery of a new class of carbon nanomaterials, such as fullerenes, graphenes, and carbon nanotubes [2–10]. The wealth of possibilities of employing constructional materials to harden constructional materials can be confirmed by a discovery made recently at Dresden University of Technology, Germany [11]. According to the results obtained via high-resolution transmission electron microscopy, Damascus steel samples taken from a museum piece (a saber produced in the sixteenth century) contain multilayer carbon nanotubes. Such an observation became possible after a small metal sample was dissolved in hydrochloric acid. The undissolved material comprised multilayer carbon nanotubes up to 5×10^{-9} m in diameter with a typical interlayer spacing close to 0.34×10^{-9} m. In the majority of nanotubes, the cavity is filled with cementite, i.e., iron carbide (Fe_3C), which, as is known, possesses increased levels of hardness and brittleness. Since the nature of the hardening effect of Damascus steel has not yet been completely explained, we can surmise its similarity to that underlying metal modification due to the introduction of carbon nanomaterials followed by treatment under pressure. It is natural to think that the above-described effect of surface hardening with the help of carbon nanomaterials is related to the fact that a certain iron-carbide variant is formed on the surface of the interface between the carbon nanostructure and metal grains as a result of heat treatment accompanying the manufacture of the corresponding sample.

Despite the existence of a substantial number of publications devoted to the problem concerning constructional-material hardening as a result of the use of nanocarbon coatings with subsequent treatment with high-intensity energy sources, studies of the dependence between the behavior of hardening and process parameters, such as the coating thickness, the energy and intensity of energy sources, and treatment duration, have not been performed to date. In this work, we investigate variations in the degree of hardening of a low-carbon steel surface due to the deposition of

Table 1. Elemental composition of a low-carbon steel plate measured via the optical emission method

Elemental composition, wt %					
C	Si	Mn	Ni	Cr	Cu
0.077 ± 0.019	0.087 ± 0.009	0.393 ± 0.008	0.011 ± 0.002	0.025 ± 0.001	0.035 ± 0.001

amorphous nanostructured carbon followed by electron-beam treatment. The findings of the investigation are compared with the results obtained when a low-carbon steel surface with an analogous coating is exposed to a pulsed laser beam.

EXPERIMENTAL

The hardening agent chosen was soot produced with the help of four-electrode high-frequency arc-discharge plasma in a helium atmosphere. In this case, the gas flow, frequency, and arc current were (0.05–0.1) × 10^{-3} m^3/s, 66 × 10^3 Hz, and 220 A, respectively [12]. The electrodes were oriented along pyramid ribs at an angle of 57°. The nanostructured carbon soot created by electric-arc sputtering was treated in a SOXHLET-type setup to extract fullerenes. After fullerene extraction, the specific surface of the soot was measured via the Brunauer–Emmett–Teller method using a Sorbi-M apparatus. Its value turned out to be (238 ± 5) × 10^3 m^2/kg. The soot was carefully crushed in a ceramic mortar with the help of a pestle, filled with o-xylene in the ratio 100 : 1 (in mass), and intermixed to obtain a homogeneous suspension. The constructional-material base was made of 2-mm-thick low-carbon steel plates with sizes of ~1.5 × 3.5 cm. The elemental composition of the plate substance was determined using the standard optical emission method (Table 1).

The plates were dipped into the suspension and then dried over 24 h in air at a temperature of 50°C.

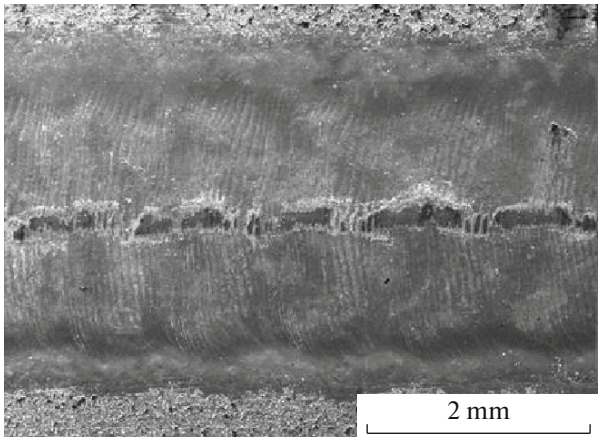

Fig. 1. SEM image of the sample surface irradiated with an electron beam. The central part of the irradiated surface exhibits a wear groove resulting from tribological tests.

With the aim of improving the adhesion thereof, they were annealed in a low argon flow (up to 1.7 × 10^{-6} m^3/s) inside a furnace for 20 min at a temperature of 600°C. The mass of the prepared film was about 4 × 10^{-6} kg, and its average thickness turned out to be 10^{-5} m, corresponding to a coating density of 800 kg/m^3.

The electron gun of an AELTK-12 setup manufactured by OAO NITI Progress having a chamber volume of 12 m^3 and an accelerating voltage of 60 × 10^3 V was employed as an electron-beam source. The beam diameter was ~5 × 10^{-4} m. The treated surface was transversely scanned with an electron beam at a frequency of 1000 Hz. The electron gun was longitudinally shifted at a speed of 5 × 10^{-2} m/s. Thus, due to electron-beam treatment, a groove 2.5 mm wide and 15 mm long appeared on the sample surface (Fig. 1). At a fixed beam-scanning rate, the surface irradiation intensity was varied because of beam-current changes in the range of 3–15 mA. Measurements demonstrated that, under electron-beam treatment, the highest effect is achieved at an irradiation energy of 460 J/cm^2. Hence, experiments were carried out in the range of 140–700 J/cm^2.

In this work, the laser irradiation of samples was employed together with the electron-beam treatment of surfaces. Laser irradiation was performed using an ALFA-200C setup based on a pulsed neodymium-glass laser with a wavelength of 1.064 × 10^{-6} m and a pulse energy of 50 J. The sample surfaces were irradiated with a technical support of Laserform Co. The laser beam was focused into a spot 3.5 × 10^{-3} m in diameter. To analyze changes in the friction coefficient and wear resistance of the sample materials, which were due to the performed laser treatment, an extended groove on the sample surface had to be created with the help of laser irradiation. The given groove was formed by spots 3.5 mm in diameter when separate laser pulses with energies of 5–30 J and durations of (1–8) × 10^{-3} s acted on the sample surface. The degrees of spot overlapping were 25, 50, and 75%.

After the samples were irradiated by beams with different intensities, their microhardness was determined via the Vickers method with the help of an Emco-Test DuraScan 20 hardness tester. In addition, the treated samples were tribologically tested to find changes in the friction coefficient. The tests were performed using a CSM Instruments SA TRB-S-CE-0000 hardness tester without lubrication at a temperature of 22 ± 2°C by means of the ball–plane method (under the condition of linear reciprocal transportation of the sample with

respect to an immovable body at a specified amplitude). Wear groove images were obtained using a Tescan MIRA 3 LMU high-resolution scanning electron microscope (SEM) with a thermal-field Schottky cathode in the reflected-electron recording mode.

It should be emphasized that different surface regions exposed to a laser pulse of a certain energy and duration manifest various degrees of modification. This is related to the fact that the laser-radiation intensity is inhomogeneously distributed over the spot surface and the structure itself has inhomogeneities. The typical SEM image of a laser-irradiated surface region with a nanocarbon coating is depicted in Fig. 2.

In measurements performed at different points of the laser spot, a spread in microhardness values is observed. This is due to the fact that the laser-radiation intensity is inhomogeneously distributed over the spot surface and the sample structure has inhomogeneities. The data from Table 2 indicate that laser irradiation of the steel surface without a nanocarbon coating can both increase and decrease the microhardness.

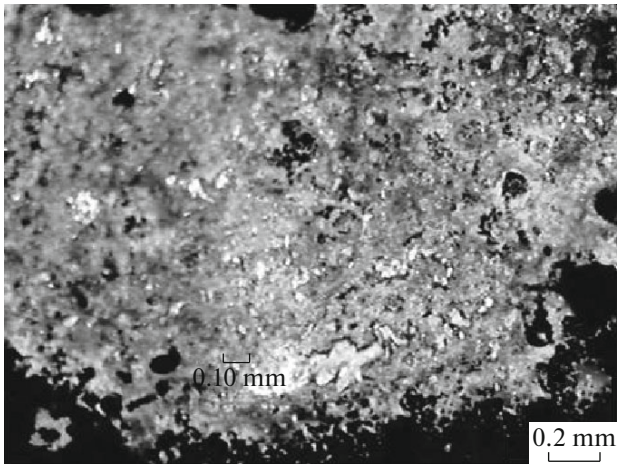

Fig. 2. Typical SEM image of a laser-irradiated surface region with a nanocarbon coating.

RESULTS AND DISCUSSION

The microhardness of the initial samples not covered with a nanocarbon coating and not subjected to electron-beam irradiation was 152 ± 12 HV. The pronounced effect of surface hardening is observed if the nanocarbon-coated surface is exposed to electron or laser irradiation. The measured microhardnesses of the given samples subjected to electron irradiation with different energy densities are depicted in Fig. 3. Their values are compared with analogous data obtained during laser irradiation of the same surface with the same type of nanocarbon coating. As is seen, the aforementioned dependences of microhardness inherent to both types of surface irradiation are nonmonotonic. The highest fourfold effect of surface hardening (on the order of 600 ± 20 HV) is attained if the electron irradiation energy is 460 J/cm^2. With the use of laser irradiation, a sevenfold effect is observed.

The microhardnesses measured along the wear groove produced by a laser beam on the nanocarbon-coated surface are compared in Fig. 4. The behavior of surface hardening becomes more homogeneous with a growing degree of overlapping of laser spots.

From a comparison between two types of high-energy sources acting on nanocarbon-coated surfaces, it can be inferred that laser treatment under optimal conditions leads to a larger increase in the surface microhardness at a smaller expenditure of energy than that achieved under electron-beam action. However, as is shown below, the measured wear resistances of the treated surface indicate that the hardened-layer thickness turns out to be greater by a factor of approximately 2.5 for electron-beam action than in the case of laser irradiation.

In revealing the degree of electron-beam action on a low-carbon steel surface with a nanocarbon coating, it is necessary to determine the heat balance under surface irradiation and estimate the relationship between the characteristic depth l_e of fast electron penetration into a material, the lateral size d_e of the electron beam, and the characteristic length l_t of thermal conductivity.

When fast electron penetration into a sample is estimated, the classical Bohr approach [13] describing how fast particles are decelerated in a material can be employed. In accordance with this approach based on

Table 2. Measured microhardnesses of the samples not covered with a nanocarbon coating and irradiated with laser pulses of a certain energy and duration

Pulse energy E, J	Pulse duration τ, ms	Comment	Microhardness, $HV_{0.01}$
9	3	Strong darkening of the entire surface	170 ± 30
5	1	Weak change in surface color	180 ± 20
9	1	Surface yellowing	320 ± 80
12	5	Edge blackening	220 ± 50

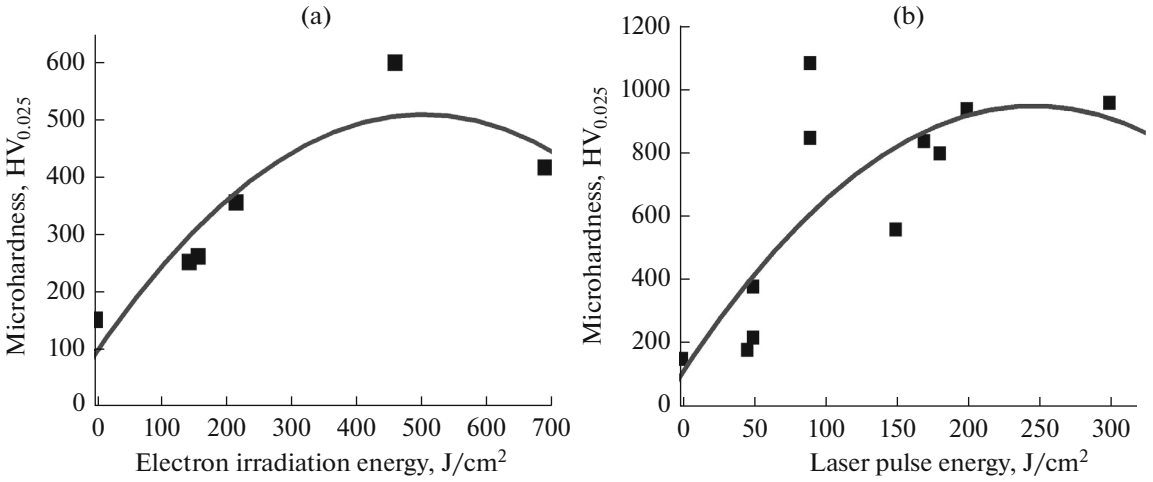

Fig. 3. Dependences of the microhardness of nanocarbon-coated steel samples on (a) electron and (b) laser irradiation energies.

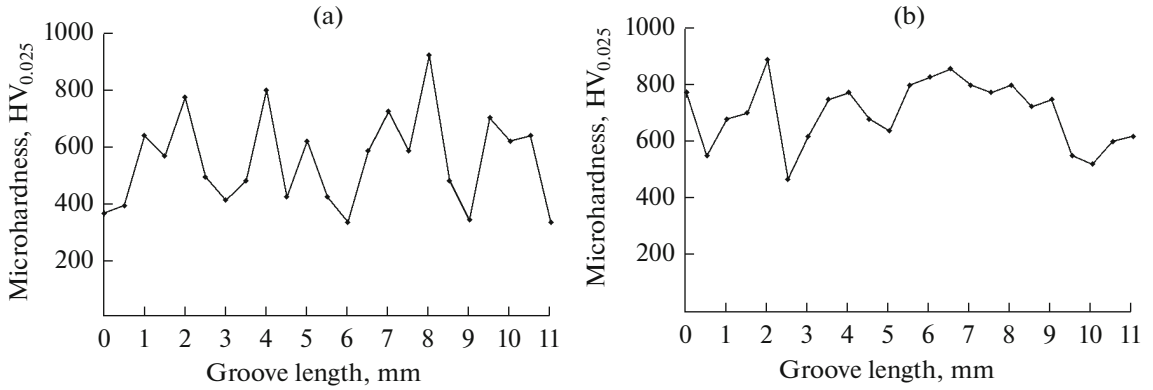

Fig. 4. Variations in the microhardness along the groove length at different degrees of overlapping of laser spots: (a) 25 and (b) 75%.

the assumption that the basic mechanism of fast particle deceleration is related to their scattering from free and bound electrons existing in the material, the energy-loss intensity is defined by the expression

$$\frac{\partial \varepsilon_e}{\partial x} = -\frac{2\pi}{\varepsilon_e} NZe^4\Lambda, \qquad (1)$$

where ε_e is the electron energy, e is its charge, N is the medium density, Z is the atomic number, $\Lambda \sim \ln(\varepsilon_e/I) \sim 10$ is the Coulomb logarithm, and I is the average electron binding energy in an atom. Integrating relationship (1), we obtain the following expression for the penetration depth of an electron with the energy ε_e in the steel sample:

$$l_e = \frac{\varepsilon_e^2}{4\pi NZe^4\Lambda}. \qquad (2)$$

The substitution of $\varepsilon_e = 96 \times 10^{-16}$ J, $Z = 26$, $N = 0.84 \times 10^{17}$ m^{-3}, and $I \sim 1.6 \times 10^{-18}$ J into (2) provides an estimate of the characteristic length of electron penetration into the material: $l_e \approx 6 \times 10^{-6}$ m. The energy released during electron-beam absorption is converted into heat and propagates along the sample thanks to thermal conductivity. When conditions are optimal (the beam current is $I \sim 10^{-2}$ A and the irradiation power is $W = IU \approx 600$ W) and an electron beam scans the surface with the rate $v_b = 5 \times 10^{-2}$ m/s, the duration of its action on the treated groove with the length $l_p = 1.5 \times 10^{-2}$ m and the width $d_p \approx 0.25 \times 10^{-2}$ m is $\tau_{es} \sim l_p/v_b \sim 0.3$ s. As a result, the surface with the area $l_p \times d_p \approx 0.37 \times 10^{-4}$ m^2 acquires the energy $Q \approx W\tau_{es} \approx 180$ J. This corresponds to an incident energy density of about 5×10^{-2} J/m^2. Due to thermal conductivity, this energy is transferred over a distance on the order of $d_t \sim (\tau_{es}\chi)^{1/2}$ during the entire duration. In this case, $\chi = \lambda/\rho C$ is the thermal diffusivity of the material, ρ is its density, C is the specific heat, and λ is the thermal conductivity coefficient. Substituting the tabulated values for steel corresponding to 1000 K, namely, $\lambda \approx 30$ W/(m K), $C \approx 0.6 \times 10^{-3}$ J/(kg K), $\rho = 7800$ kg/m^3 [14], we obtain $\chi \approx 0.06 \times 10^{-4}$ m^2/s and

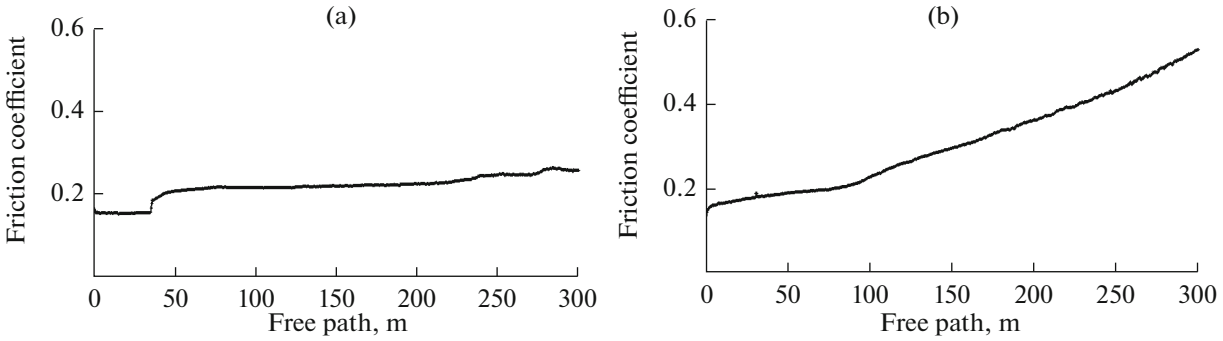

Fig. 5. Dependences between the friction coefficient and the free path for a sample subjected to (a) electron and (b) laser treatments.

$d_t \sim 0.1 \times 10^{-2}$ m. This implies that, upon completion of the action of the beam, the volume occupied by the energy absorbed in the material is approximately $V = l_p d_p d_t \sim 0.04 \times 10^{-6}$ m^3. Hence, the material of the given volume is heated by the quantity

$$\Delta T_{\max} \approx \frac{Q}{C\rho V}. \quad (3)$$

Substituting the quantities estimated above ($V = l_p d_t d_p \sim 3.7 \times 10^{-9}$ m^3, $Q = 180$ J, $C \approx 0.6 \times 10^{-3}$ J/(kg K), and $\rho = 7800$ kg/m^3) into (3), we arrive at $\Delta T_{\max} \approx 950$ K. It is pertinent to note that the energy required to melt the material of the region under consideration, $Q_m = C_m V \rho$, is less than 10 J, constituting only a negligible part of the total energy absorbed by the sample. Here, $C_m = 78 \times 10^3$ J/kg is the specific melting heat of iron. Thus, practically the entire absorbed energy is converted into heat.

Since the performed estimation is rough, i.e., is valid to within several tens of percent, the observed signs of surface melting of the irradiated sample enable us to infer that, due to electron-beam treatment, its near-surface region several microns thick is heated to a temperature exceeding the melting point $T_m \approx 1800$ K. In accordance with the features of thermal conductivity, the temperature smoothly decreases with distance from the heat release region whose thickness is estimated as 6×10^{-6} m. In the melting region of the material, intense convection occurs, due to which carbon nanoparticles penetrate from the surface to a depth of several tens of microns.

Table 3. Measured friction coefficients

Region	Friction coefficient μ		
	initial	intermediate	final
Electron-beam treatment	0.14	0.195	0.25
Laser-beam treatment	0.14	0.3	0.54
Without treatment	0.20	0.4	0.66

In determining changes in the friction coefficient and wear resistance of sample materials arising from the performed electron-beam treatment, it was required to create an extended groove on the sample surface. Such a groove 2.5 mm wide and 15 mm long is generated when the surface is scanned by an electron beam at the scanning parameters described above (Fig. 1). Friction tests were carried out within the given groove. The dependences between the friction coefficient μ and the friction length L, which were measured under electron-beam and laser treatment of the sample, are depicted in Figs. 5a and 5b, respectively.

The friction coefficients obtained during tribological tests are presented in Table 3. As is evident from analysis of the tribological test results, the friction coefficient of the treated surface is 20–30% lower than that of the initial sample surface. A gradual increase in the friction coefficient observed during tests can be related to the fact that the groove depth, as well as the ball area contacting with the material surface, increases and the modified layer with a gradient of properties over depth is removed little by little during wearing. It is clearly seen from Fig. 5a that the modified-layer thickness corresponding to electron-beam irradiation is considerably greater than that inherent to laser treatment.

CONCLUSIONS

The main result of this work is the experimentally revealed effect of steel-surface hardening arising from nanocarbon-material deposition with subsequent treatment by high-intensity particle beams. The measurements indicate the nonmonotonic dependence between the degree of hardening and the beam intensity. In other words, the experimental results demonstrate that the observed effect can be optimized. The degree and behavior of hardening can depend on both the type of nanocarbon coating and the high-energy action method. With the aim of developing the described approach, nanocarbon materials, such as graphene, fullerenes, and carbon nanotubes, are further planned to be employed as coatings. Moreover,

high-power ion beams and heating under pressure can be proposed as high-energy sources affecting the nanocarbon coated surface. Since all approaches mentioned above require optimization, future experiments must be performed in a wide range of parameters (coating thickness, intensity, nature of action).

ACKNOWLEDGMENTS

This study was supported by the Russian Science Foundation, project no. 16-19-10027.

REFERENCES

1. V. M. Prikhod'ko, L. G. Petrova, and O. V. Chudina, *Metallic and Physical Foundations of Strengthening Technologies* (Mashinostroenie, Moscow, 2003) [in Russian].
2. A. V. Eletskii, Usp. Fiz. Nauk **177** (3), 233 (2007).
3. O. Chernogorova, E. Drozdova, I. Ovchinnikova, A. Soldatov, and E. Ekimov, J. Appl. Phys. **111–112**, 601 (2012).
4. O. P. Chernogorova, E. I. Drozdova, V. M. Blinov, and I. N. Ovchinnikova, Russ. Metall. (Engl. Transl.) **2011** (3), 221 (2011).
5. O. P. Tchernogorova, O. A. Bannykh, V. M. Blinov, E. I. Drozdova, A. A. Dityat'ev, and N. N. Mel'nik, Mater. Sci. Eng. **299**, 136 (2001).
6. E. I. Drozdova, O. P. Chernogorova, T. I. Borodina, and V. V. Milyavskiy, Fullerenes, Nanotubes, Carbon Nanostruct., Nos. **5–6**, 301 (2008).
7. O. P. Chernogorova, E. I. Drozdova, V. M. Blinov, and N. A. Bul'enkov, Nanotechnol. Russ. **3** (5–6), 344 (2008).
8. S. R. Bakshi, D. Lahiri, and A. Agarwal, Int. Mater. Rev. **55** (1), 41 (2010).
9. K. T. Kim, S. I. Cha, S. H. Hong, and S. H. Hong, Mater. Sci. Eng. **430**, 27 (2006).
10. Annual Report of Fraungofer Institute for Manufacturing Engineering and Automation IPA. 01.2013. http://www.energie.fraunhofer.de/en/bildmaterial/flyer_hannover-messe/ipa-fraunhoferinstitute-formanufacturing-engineering-and-automation/ipa-metal-matrix-composites.
11. M. Reibold, P. Paufler, A. Levin, W. Kochmann, N. Pätzke, and D. C. Meyer, Nature **444**, 286 (2006).
12. G. N. Churilov, N. G. Vnukova, A. I. Dudnik, G. A. Glushchenko, I. A. Dubinina, U. E. Gulyaeva, A. A. Popov, and N. A. Samoylova, Tech. Phys. Lett. **42** (5), 475 (2016).
13. Yu. M. Shirokov and N. P. Yudin, *Nuclear Physics* (Nauka, Moscow, 1972) [in Russian].
14. *Physical Quantities. Handbook,* Ed. by I. S. Grigor'ev and E. Z. Meilikhov (Energoatomizdat, Moscow, 1991) [in Russian].

Translated by S. Rodikov